

A comparative evaluation of the parallel flow and spherical reservoir models of HDR geothermal systems

Derek Elsworth¹

Waterloo Centre for Groundwater Research, University of Waterloo, Waterloo, Ont. N2L 3G1, Canada

(Received September 22, 1989; revised and accepted April 13, 1990)

ABSTRACT

Elsworth, D., 1990. A comparative evaluation of the parallel flow and spherical reservoir models of HDR geothermal systems. *J. Volcanol. Geotherm. Res.*, 44: 283–293.

A terminology is developed to link two conceptual semi-analytical models of HDR geothermal energy extraction through the common criterion of reservoir volume. The first is a parallel fracture model (PFM) that represents thermal recovery from an arrangement of prismatic blocks, thermally isolated from the geologic host medium. The second is a spherical reservoir model (SRM) that admits energy recovery from both a central production zone and the surrounding geologic body. Behaviour of the two different, but complementary, systems are governed by the dimensionless variables of thermal drawdown, T_D , circulation rate, Q_D and time, t_D , with the PFM further conditioned by a diffusion length ratio representative of the fracture spacing. Thermal response of the PFM exhibits a worst case threshold for thermal recovery at small magnitudes of circulation rate Q_D , corresponding to the system progressing in near thermal equilibrium. A close correspondence exists between the thermal response of the PFM for low Q_D and that of the SRM for high Q_D where the influence of external heat supply is not apparent. Circulation tests conducted in existing reservoirs return magnitudes of Q_D and diffusion length ratios that suggest they are operating close to thermal equilibrium as predicted from the PFM. With this determined "a priori", the assumptions made in the SRM are not violated, suggesting the significant contribution that external heat supply may make to the gross energy recovery. As predicted by the SRM, energy recovery remains practically unbounded for relevant magnitudes of Q_D with this effect being noticeable well within the projected reservoir lifetime.

Introduction

Hot Dry Rock (HDR) geothermal energy production has been proposed as a viable method of recovering geologic thermal energy. Viability is controlled by the economics of production. The high capital costs required to develop an HDR reservoir must be amortized over the useful and productive lifetime. For this reason, a key question in establishing the

economic viability, in addition to the necessary establishment of a low-impedance hydraulic link, is the gross thermal recovery that may be anticipated. Conceptual models representing the essential physics of the HDR problem have been proposed, appropriately simplified to render the problem tractable. Of critical importance in their applicability to realistic energy recovery prediction are the restrictions posed by the simplifying assumptions. The attributes of, and predictions from, two contrasting models are critically examined in the following. The first is a multiple parallel fracture model (PFM) assuming plane flow across a volume of rock that is thermally de-

¹Present Address: Department of Mineral Engineering, Pennsylvania State University, University Park, PA 16827, U.S.A.

tached from the host geologic medium (Gringarten and Witherspoon, 1973; Gringarten et al., 1975) and therefore admits no further heat supply from the surrounding rock. The second is a thermal drawdown model accommodating heat supply from the external geologic host to a spherical production zone (Elsworth, 1989a, b), in which the circulating fluid and rock are assumed in thermal equilibrium. This model is referred to in the following as the spherical reservoir model (SRM).

The two models are semi-analytical and represent continuum behaviour of the reservoir or a representative portion of the reservoir. Spatial heterogeneities or developing flow heterogeneities within the reservoir that may be represented through complex numerical simulators are not, by definition, represented. Conversely, lumped parametric evaluation of reservoirs is viewed as an indispensable alternative in the "data poor" subsurface environment. It is in this simplified context that the following is presented.

To facilitate a comparison between the thermal outputs and drawdowns in the two geometrically different but comparable systems, a common terminology must be developed. Against this background, the limitations of the two models in predicting realistic behaviour may be highlighted.

Comparative analysis

Both models are linear, requiring that the physical constants and geometry remain constant in time. In a common terminology, the specific heat capacities of the circulating fluid ($\rho_F c_F$) and rock ($\rho_R c_R$) and the thermal conductivity of the intact rock (K_R) are invariant. Fluid temperatures are defined at inlet (T_{Fi}) and outlet (T_{Fo}) with the initial rock temperature (T_{R0}) assumed constant over the depth of the reservoir. Apart from these common phenomenological components, the specific geometries of the two models differ considerably and must be separately stated.

Parallel fracture model (PFM)

The geometry of the parallel fracture model is characterized as a periodic arrangement of prismatic rock blocks separated by fractures of uniform aperture and, therefore, identical flow and transport characteristics. As illustrated in Figure 1, the prismatic blocks are of thickness x_E , height z_E , and out of plane width y_E . Initially the system is in thermal equilibrium at temperature T_{R0} . A linear flow is introduced in all fractures, of summed volumetric flow rate per unit width per unit time given by Q . Fluid is injected at constant temperature T_{Fi} and withdrawn at the fracture top at, initially unknown, temperature T_{Fo} . Heat supply from the rock to the fluid is by one-dimensional conduction in the x direction. The most significant attribute of the model is that it accounts for spatial change of fluid and rock temperatures along the fracture (z direction). Our interest is restricted to the magnitude of the outlet temperature T_{Fo} .

Where the geothermal gradient is assumed constant over the fracture height (z_E), behaviour of the system is controlled by the three modified dimensionless parameters:

$$T_D = \frac{\langle T_{Fi} - T_{Fo} \rangle}{(T_{Fi} - T_{R0})} \quad (1)$$

$$X_{ED} = \left(\frac{\rho_F c_F}{K_R} \right) \left(\frac{Q}{z} \right) z_E \quad (2)$$

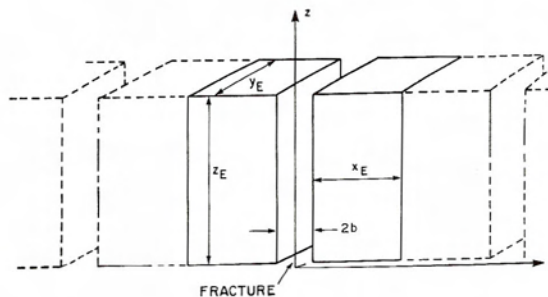


Fig. 1. Repeating geometry of the Parallel Fracture Model (PFM) for geothermal energy extraction.

$$t'_D = \left[\frac{(\rho_F c_F)^2}{K_R \rho_R c_R} \right] \left(\frac{Q}{z} \right)^2 t' \quad (3)$$

where t' is real time following breakthrough of the hydrodynamic front given as $t' = t - (z/v_F)$ where v_F is the flow velocity within the fracture. For all practical purposes, $t' \approx t$ where the time scales of interest extend over the productive lifetime of the system. The initial rock temperature is given as T_{R0} .

Spherical reservoir model (SRM)

The spherical reservoir model differs from the parallel fracture model in that it assumes a simplified mechanism for heat extraction from the spherical thermal core as illustrated in Figure 2. Fluid is injected at constant volumetric flow rate q_F , at temperature T_{Fi} and withdrawn at temperature T_{Fo} . The initial rock temperature is assumed constant and of magnitude T_{R0} . No spatial dependence is assumed in fluid temperature within the spherical production zone, of radius a . The analysis assumes the circulating fluid to be in thermal equilibrium with the rock comprising the spherical production zone. Thermal drawdown within the spherical zone induces conductive energy supply from the surrounding medium. The magnitude and temporal distribution of this secondary supply is deter-

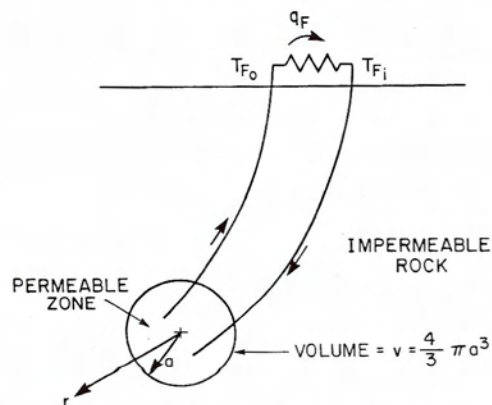


Fig. 2. Geometry of the Spherical Reservoir Model (SRM) for geothermal energy extraction.

mined by solution of the spherical boundary value problem with $T_R(\infty, t) = T_{R0}$ and $T_R(a, t) = T_{Fo}$. Considering only the case where energy is recovered from an infinite medium, the behaviour is represented by the four dimensionless parameters:

$$T_D = \frac{< T_{Fi} - T_{Fo} >}{(T_{Fi} - T_{R0})} \quad (4)$$

$$Q_D = \frac{q_F \rho_F c_F}{K_R a} \quad (5)$$

$$\Phi_D = \frac{\rho_S c_S}{\rho_R c_R} \quad (6)$$

$$t_D = \frac{K_R t}{\rho_R c_R a^2} \quad (7)$$

where $\rho_S c_S = \rho_R c_R (1 - \phi) + \rho_F c_F \phi$ and represents the aggregated thermal capacity of the material present in the spherical production zone of secondary porosity, ϕ . For practical purposes, Φ_D is expected to vary between 1 and approximately 1.1; a range in which solution is not sensitive to the parameter. For this reason, attention will focus on behaviour of the three remaining parameters as $\Phi_D = 1.0$.

Unified statement

Thermal histories predicted by the parallel fracture and spherical reservoir models may be compared if a common dimensionless terminology is used to represent both the time dimension and the fluid circulation rate. A natural bias of the author is to retain use of the dimensionless circulation rate (Q_D) and dimensionless time (t_D) parameters given in equations (5) and (7), respectively, and appropriately transform X_{ED} and t'_D of equations (2) and (3). A necessary initial step is to define common flow rates for each of the models. For a total of n fractures comprising the PFM, the equivalent flow rate for a fracture of out of plane width y_E is given as:

$$nQy_E = q_F \quad (8)$$

Similarly, since the geometries of the two models differ significantly, a common reservoir volume (v) may be defined to facilitate cross comparisons. Equating the volumes of the parallel fracture and spherical reservoirs, respectively, yields:

$$v = 2n(x_E y_E z_E) = \frac{4}{3} \pi a^3 \quad (9)$$

where q_F and v are chosen as the common variables comprising total flow rate and total reservoir volume, respectively, the dimensionless variables representing the two models may be reformed. For the SRM, the dimensionless variables become:

$$Q_D = \frac{q_F \varrho_F c_F}{K_R a} = \frac{q_F \varrho_F c_F}{K_R} \left(\frac{4\pi}{3v} \right)^{1/3} \quad (10)$$

$$t_D = \frac{K_R t}{\varrho_R c_R a^2} = \frac{K_R t}{\varrho_R c_R} \left(\frac{4\pi}{3v} \right)^{2/3} \quad (11)$$

and for the PFM:

$$X_{ED} = 2Q_D \left(\frac{3}{4\pi} \right)^{1/3} \left(\frac{z_E}{v^{1/3}} \right)^2 \quad (12)$$

$$t'_D = X_{ED}^2 t_D \left(\frac{3}{4\pi} \right)^{2/3} \left(\frac{v^{1/3}}{x_E} \right)^2 \quad (13)$$

where it is apparent that an extra geometric term $x_E/v^{1/3}$ has emerged to represent the "shape" or "thermal drawdown potential" of the reservoir. Otherwise, the behaviour of both systems may be rigorously stated in terms of T_D, Q_D, t_D , and $(x_E/v^{1/3})$.

Thermal drawdown behaviour

The assumptions applied to the SRM result in thermal drawdown T_D being a unique function of t_D for various circulation rate magnitudes, Q_D . Similar behaviour is ap-

parent in the PFM where performance is further regulated by the shape parameter $(x_E/v^{1/3})$. To compress the temporal results onto a suitable scale for graphical representation, the PFM (Gringarten and Witherspoon, 1973) has used real time premultiplied by Q_D^2 [as given in equation (12)] and the SRM has used real time premultiplied by Q_D (Elsworth, 1989). In choosing the latter of these representations for all future data, the parameters t'_D and X_{ED} from the PFM may be transformed as:

$$Q_D = \frac{1}{2} X_{ED} \left(\frac{4\pi}{3} \right)^{1/3} \left(\frac{v^{1/3}}{x_E} \right)^2 \quad (14)$$

directly from equation (12) and:

$$Q_D t_D = \frac{2\pi}{3} \frac{t'_D}{X_{ED}} \quad (15)$$

from substituting equation (12) into equation (13) and premultiplying by equation (14). With this correspondence established, results from the two complementary analyses may be directly contrasted.

Results are illustrated as a function of modified dimensionless time $Q_D t_D$ for different shape factors $(x/v^{1/3})$ in Figures 3a through 3c for the PFM and in Figure 4 for the SRM. Available data from the Los Alamos Fenton Hill reservoir and the Camborne Geothermal Energy Project reservoir each suggest reservoir volumes of the order of $4 \times 10^6 \text{ m}^3$. Assuming the diffusion length, x_E , separating adjacent flow paths to be of the order of 10 m returns a dimensionless shape factor, $x/v^{1/3}$, of 6.2×10^{-2} . Thus, Figures 3a through 3c bracket the anticipated range of values, with $x/v^{1/3} \ll 1.0$.

The PFM predicts a rapid initial drop in production temperature from the system for large circulation rates Q_D . For large Q_D , a longer tail to the depletion process is evident as thermal drawdown covers an increased timespan. Physically, this corresponds to rapid cooling of the rock close to the fracture flow path,

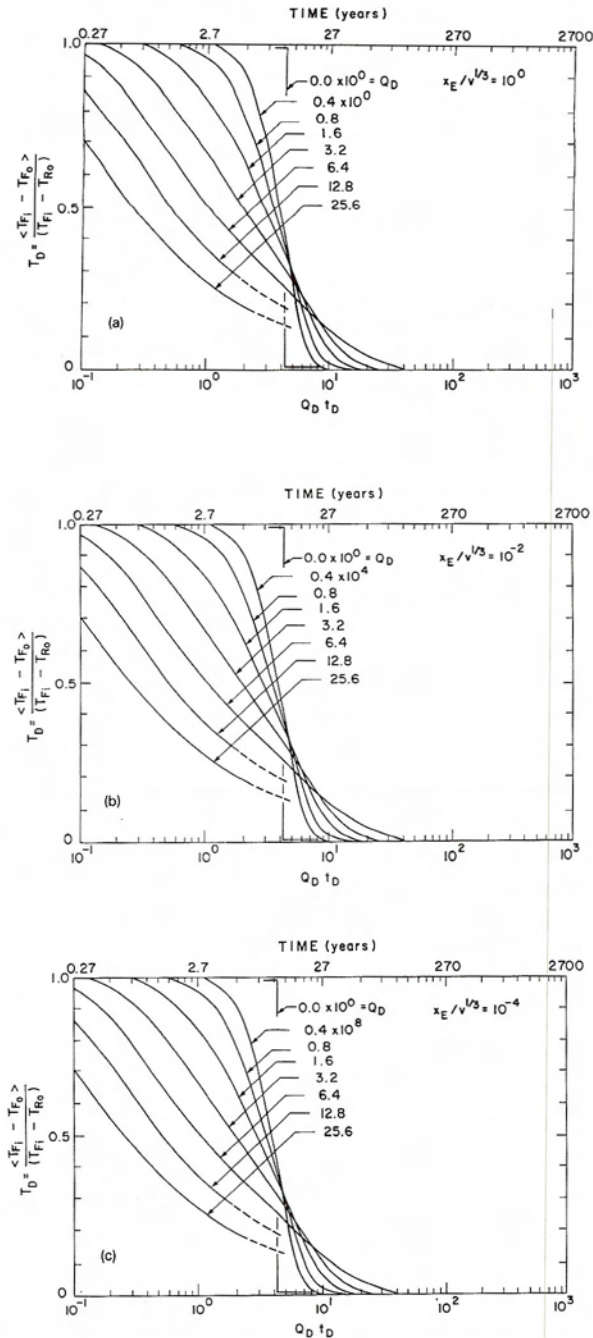


Fig. 3. Thermal drawdown rates (T_D) for the Parallel Fracture Model representing diffusion length ratios of (a) $x_E/v^{1/3} = 1.0$; (b) $x_E/v^{1/3} = 10^{-2}$; (c) $x_E/v^{1/3} = 10^{-4}$. Upper time scale in years is evaluated specifically for $Q_D = 10^2$.

where the diffusion length is small, followed by a less rapid thermal drawdown of the interior. As Q_D is decreased, corresponding to a high thermal conductivity or low circulation rate, the thermal drawdown process within the rock becomes more uniform. The high thermal conductivity of the rock allows rapid heat supply to the fracture but the low circulation rate, or conversely, the low specific heat capacity of the fluid ($\rho_F c_F$) is unable to remove the thermal energy with commensurate rapidity. This latter condition for low relative Q_D values corresponds to a state of thermal equilibrium being maintained between the spatially uniform fluid and rock temperatures.

For small magnitudes of Q_D , the PFM duplicates one of the primary assumptions of the SRM, namely, the requirement for thermal equilibrium between the rock and the circulating fluid. The threshold behaviour for small Q_D from the PFM (represented by $Q_D = 0.0$ in Figure 3a and similarly in 3b and 3c) is similar to the response of the SRM at very large magnitudes of Q_D as illustrated in Figure 4. This bounding behaviour in the SRM represents the situation where thermal recharge from the surrounding geologic medium is inconsequential as a result of high fluid circulation rates. The slight mismatch between the two threshold behaviours results from the incorporation of spatial variation in fluid temperature T_F between inlet and outlet, a factor that is neglected in the SRM. This inconsistency in assumptions results in a steeper decline for the PFM over the SRM with the decline initiating later but concluding more prematurely. Thus, it may be concluded that the neglecting of spatial temperature variation in the SRM has the net effect of diffusing the temperature decline slightly throughout time but that the overall timing of the depletion remains relatively accurate. The time to 50% thermal drawdown predicted by the PFM and the SRM are essentially coincident, for the limiting behaviours. This finding is of considerable im-

portance since it suggests that overall geometry of the reservoir is of secondary importance to reservoir volume providing the magnitudes of Q_D fall within a certain range.

The range of magnitudes of Q_D , over which the responses of the PFM and SRM return similar results, is controlled exclusively by the diffusion length ratio $x_E/v^{1/3}$. As the diffusion length ratio decreases, this threshold behaviour is realized for increasingly larger circulation rates. Physically, this represents an increase in efficiency with which the reservoir rocks are able to shed heat. This may correspond to a greater number of flow paths traversing the rock volume. Since thermal diffusion rate is directly proportional to the diffusion length (x_E) raised to the power two, the increase in initial thermal efficiency of the system would be anticipated.

The further attribute of the SRM is the ability to evaluate the thermal contribution of the medium immediately surrounding the reservoir zone. As illustrated in Figure 4, where Q_D decreases below 10^2 , this contribution becomes significant at large dimensionless times and may therefore make a positive contribution in determining the economic viability of the system. Naturally, for this to be the

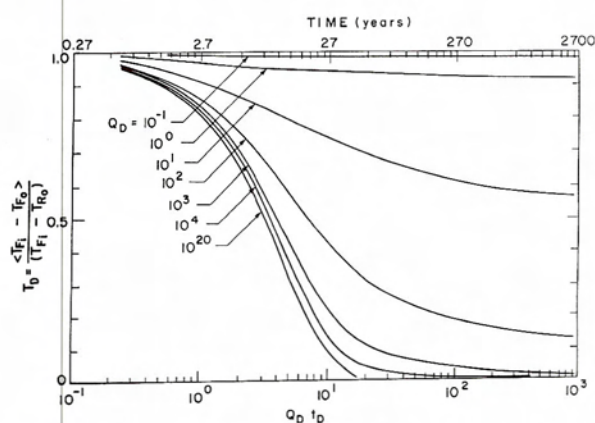


Fig. 4. Thermal drawdown rates (T_D) for the Spherical Reservoir Model. Upper time scale in years is evaluated specifically for $Q_D = 10^2$.

case, the projected lifetime of the energy project must be sufficient to benefit from this yield. This factor will be discussed later.

Energy output

The critical parameters in establishing viability of any prospective HDR site are the magnitude and rate of thermal energy production that may be stimulated. The cumulative thermal energy production at any time t is given as $H(t)$, allowing the production to be normalized with respect to the total cumulative thermal energy production as $H(t)/H(\infty)$. For the PFM, where the extraction zone is thermally detached from the exterior, the ratio $H(t)/H(\infty)$ asymptotes to unity as $Q_D t_D \rightarrow \infty$. This is illustrated in Figures 5a through 5c. As a natural consequence of the similarity in the drawdown curves of Figures 3a through 3c, the normalized energy recovery rates are also fixed in $Q_D t_D$ space. Again, the corresponding magnitudes of Q_D that precipitate the threshold behaviour are controlled by the diffusion length ratio, $x_E/v^{1/3}$.

The most rapid energy depletion in $Q_D t_D$ space is given for the PFM as Q_D decreases. This represents the most efficient energy withdrawal as the residence time within the reservoir is sufficiently large to enable the circulating fluid to be fully charged with thermal energy. This response is the corollary of the system maintained at thermal equilibrium, indicative of low Q_D magnitudes. Although this is the optimal rate of thermal energy extraction with minimized fluid circulation costs, it does not result in the most rapid acquisition of energy from the system. At the other extreme, the slowest energy recovery response is returned as $Q_D \rightarrow \infty$.

Energy output from the SRM may similarly be evaluated. The limiting values corresponding to $Q_D \rightarrow 0$ yield threshold behaviours in $Q_D t_D$ space. Cumulative thermal energy production is given by:

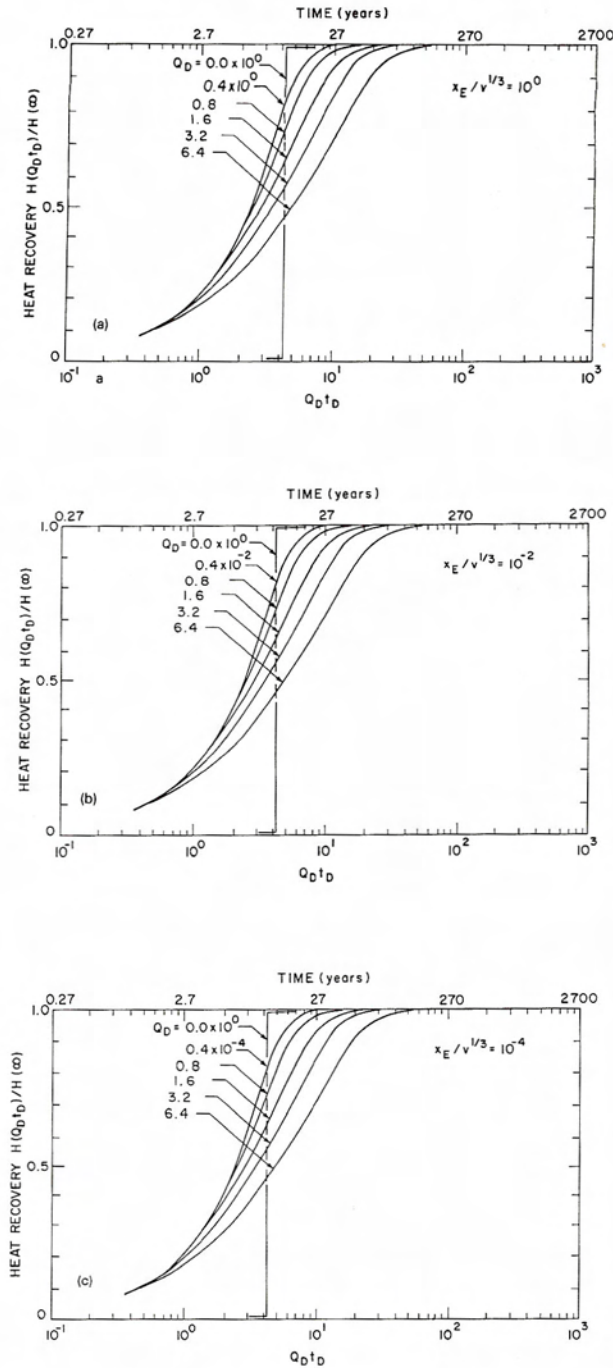


Fig. 5. Cumulative energy recovery rates $H(t)/H(\infty)$ for the Parallel Fracture Model representing diffusion length ratios of (a) $x_E/v^{1/3} = 1.0$; (b) $x_E/v^{1/3} = 10^{-2}$; (c) $x_E/v^{1/3} = 10^{-4}$. Upper time scale is evaluated specifically for $Q_D = 10^2$.

$$H(t) = \int_0^t q_F \rho_F c_F < T_{F_0} - T_{F_i} > dt \quad (16)$$

where, from equation (1), $< T_{F_0} - T_{F_i} > = T_D(T_{R_0} - T_{F_i})$. For the SRM, (Elsworth, 1989) it may be shown that the threshold behaviour for large Q_D , illustrated in Figure 4, is given by $T_D = \exp(-3Q_D t_D/4\pi)$ which, following substitution into equation (16) and integration, yields:

$$H(t) = \frac{4\pi}{3Q_D} \frac{\rho_R c_R a^2}{K_R} q_F \rho_F c_F (T_{R_0} - T_{F_i}) [1 - \exp(-3Q_D t_D/4\pi)] \quad (17)$$

The magnitude of the total thermal energy production may be recovered from equation (17) as $t_D \rightarrow \infty$, returning the normalized energy production history as:

$$H(t)/H(\infty) = 1 - \exp(-3Q_D t_D/4\pi) \quad (18)$$

Where Q_D is very small, the thermal drawdown is minimal as evident from Figure 4. Thus, assuming $< T_{F_0} - T_{F_i} > = (T_{R_0} - T_{F_i})$ corresponding to $T_D(t_D) = 1$ for $Q_D \rightarrow 0$ and substituting this into equation (16) yields, following integration:

$$H(t)/H(\infty) = 3Q_D t_D/4\pi \quad (19)$$

where $H(\infty)$ is evaluated from equation (17), corresponding to the fully insulated reservoir.

Although, rigorously, equations (18) and (19) represent behaviour in the limits as $Q_D \rightarrow \infty$ and $Q_D \rightarrow 0$, respectively, the realistic bounds to the parameter Q_D are relatively narrow. From the asymptotic behaviour evident in Figure 4, the bounds on energy production are controlled by $Q_D > 10^4$ as the uppermost production rate and $Q_D < 10^{-1}$ as the lowermost. Outside these bounds, the behaviour conforms to the limiting cases. The limiting energy recovery rates for the SRM are illustrated in Figure 6 where, as a natural consequence of $T_D(t)$ being uniquely defined in $Q_D t_D$ space, equations (18) and (19) are

similarly constrained.

The relatively narrow band occupied by the energy recovery histories from the SRM is interestingly embedded within the range of recovery rates recovered from the PFM. The band of variation is somewhat narrower for the SRM over the PFM due to the initial assumption made in the SRM that the reservoir remains in thermal equilibrium. The requirement ensures the the SRM system acts as a more efficient thermal engine precipitating an earlier thermal recovery for large Q_D over the case of the PFM. However, although the heat recovery ratio is bounded by $H(t)/H(\infty) = 1$, for very large magnitudes of Q_D , no such limit is imposed as Q_D decreases below approximately $Q_D < 10^4$. For small Q_D , the energy recovery ratio $H(t)/H(\infty)$ remains unbounded, reinforcing the important thermal contribution that the reservoir exterior may make to overall system performance.

As noted previously with regard to thermal drawdown, energy recovery from the PFM is controlled by the diffusion length ratio $x_E/\nu^{1/3}$. This concern is apparently less critical for the evaluation of energy recovery rates since the behaviour occupies a relatively narrow band in dimensionless time, $Q_D t_D$. However, as $x_E/\nu^{1/3}$ decreases, the threshold magnitudes of Q_D increase in direct proportion to $(x_E/\nu^{1/3})^2$ as evidenced in Figures 5a through 5c.

Real time behaviour

In light of the foregoing, it is important to contrast the performance of the two models in real time for reasonable and realistic parameter magnitudes. Circulation rates of the order $Q_D = 10^2$ (Elsworth, 1989b) have been sustained and may be expected to comprise a lower limit for future prototype schemes. Further requiring a diffusion length ratio of $x_E/\nu^{1/3} \approx 10^{-2}$ allows the thermal drawdown behaviour and energy recovery behaviour to be predicted from Figures 3b and 4 or Figures

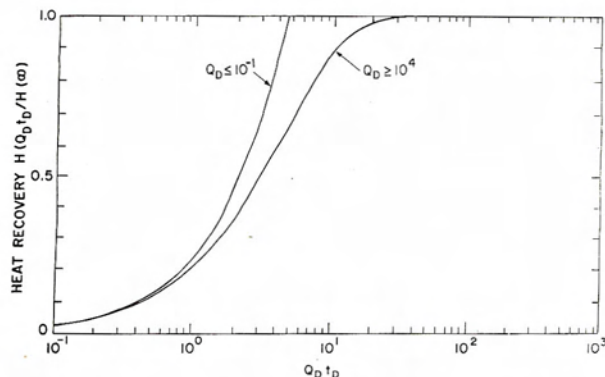


Fig. 6. Cumulative energy recovery rates $H(t)/H(\infty)$ for the Spherical Reservoir Model. Upper time scale in years is evaluated specifically for $Q_D = 10^2$.

5b and 6, respectively. For $Q_D = 10^2$, the time scales are also marked in real time, spanning the range 0.27 years to 2700 years.

The PFM predicts a reduced thermal drawdown rate over the SRM in the short term that eventually accelerates to give greater thermal drawdown in the long term. For the assumed geometric parameters representing the reservoir, it is important to note that thermal supply from the exterior has a significant effect within the prospective lifetime of an HDR project ($t < 30$ to 60 years). This is apparent in Figure 4 but more obvious in Figure 6 where thermal energy output is quantified. This observation has important ramifications in determining the viability of prospective HDR geothermal energy recovery schemes.

HDR data

The two proposed models may be compared against the measured performances of existing HDR reservoirs where long-term circulation data are available. Two potential sites are the Fenton Hill Reservoir at Los Alamos Scientific Laboratory in the United States and the Rosemanowes Reservoir at the Camborne Geothermal Project in the United Kingdom. The most important component required in

the circulation experiments is that significant thermal drawdown is obtained, thus requiring necessarily long circulation periods. Two circulation tests that meet these requirements are the 75-day circulation test at Fenton Hill (Tester and Albright, 1979; Armstead and Tester, 1987) and the 1000-day circulation test at the Rosemanowes Reservoir (Nicol and Robinson, in press).

Parameter estimation using both of these data sets may be accomplished through simple type curve matching using the following procedure:

(1) From known injection temperature, T_{Fi} , initial in situ rock temperature, T_{R0} , and measured withdrawal temperature, T_{Fo} , dimensionless temperature, T_D , may be directly evaluated against log real time, t .

(2) From curve matching against Figures 3 or 4, identify a match point in time corresponding to $t_D Q_D = 1.0$.

(3) From an estimated ratio of $\rho_R c_R / \rho_F c_F$, t corresponding to $t_D Q_D = 1.0$ and known circulation rate, q_F , evaluate the equivalent reservoir radius, a , as the parameter of greatest uncertainty, i.e.:

$$a = \left(\frac{\rho_F c_F}{\rho_R c_R} q_F t \right)^{1/3}$$

Effective reservoir volume may be recovered as $v = (4\pi/3)a^3$.

(4) From the estimated reservoir radius, a , and volume, v , dimensionless circulation rate, Q_D , may be directly recovered from equation (10) for the SRM and the PFM to check the adequacy of the curve fitting procedure of step 1. For the SRM, this merely acts as a check on the adequacy of the model. For the PFM, the final check on Q_D may be used to directly determine the reservoir shape factor, $x_E/v^{1/3}$, and hence fracture spacing.

(5) In the case of the SRM, the magnitude of Q_D should be checked to determine whether it is sufficiently low ($Q_D \leq 10^2$ or 10^3) that the assumption of thermal equilibrium in the

reservoir is met.

The previously outlined procedure is used to examine circulation data from the 75-day Fenton Hill and 1000-day Rosemanowes circulation tests. The results are illustrated in Figures 7 and 8 for the PFM and SRM, respectively. From the Fenton Hill data, the zone radius, a , is independently evaluated at 19 metres. This is considerably smaller than the interwell spacing but of comparable dimension to the zone of measured thermal depletion (e.g. fig. 10.35, p. 303, Armstead and Tester, 1987). Dimensionless circulation rate, Q_D , evaluated from the reservoir volume, v , is estimated to be $Q_D = 1.24 \times 10^3$ and compares favourably with the magnitudes identified in the SRM of Figure 8. These data for the Fenton Hill Reservoir also fit the PFM as illustrated in Figure 7 excepting the late time drawdown which is poorly reproduced. As noted in Figures 3a through c, the magnitudes of the circulation rate, Q_D , for the PFM of Figure 7 may be adjusted by considering different $x_E/v^{1/3}$ magnitudes.

The Rosemanowes Quarry Reservoir data is also illustrated on Figures 7 and 8. It should be noted that the symbols do not identify specific data points. Although run for 1000 days, the effective reservoir is considerably

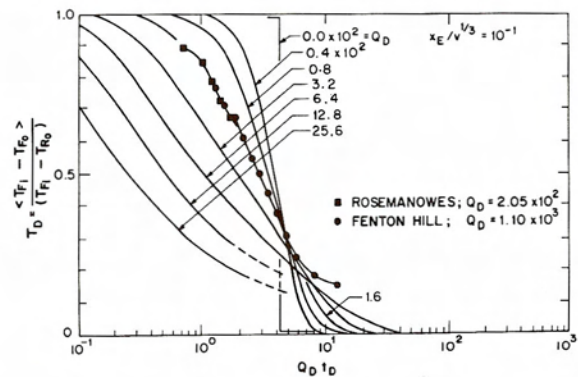


Fig. 7. Thermal drawdown data for the 75-day Fenton Hill and 1000-day Rosemanowes Quarry circulation tests compared against the Parallel Fracture Model, $x_E/v^{1/3} = 10^{-1}$.

larger than the Fenton Hill Run Segment 2 reservoir and the ultimate thermal drawdown is correspondingly lower. The SRM predicts an equivalent reservoir radius of $a = 9$ m that corresponds reasonably to the microseismic cloud observed at the site. The independently evaluated dimensionless circulation rate is $Q_D = 2.3 \times 10^2$, corresponding closely to the temporal response observed in Figure 8. The PFM also adequately represents the observed data and may be adjusted to provide a match between observed and measured dimensionless circulation.

Unfortunately, the 1000-day circulation test did not continue sufficiently long to yield definitive conclusions regarding the ultimate long-term behaviour with regard to thermal resupply from the geologic host. However, the dimensionless circulation rate, Q_D , is sufficiently low that external supply may be anticipated.

Conclusions

The similarities between the PFM and SRM have been identified under a specific range of dimensionless circulation rate magnitudes, Q_D . An equivalent response is returned for small magnitudes of Q_D in the case of the PFM

and for large Q_D magnitudes in the case of the SRM. This discrepancy in behaviour is due to the different physical assumptions that control the response of the two models. For small magnitudes of dimensionless circulation rate, the PFM progresses in a state of near thermal equilibrium between the rock and the circulating fluid. This condition is a primary assumption of the SRM but thermal signatures are only similar to the PFM where the circulation rate (in the SRM) is sufficiently high that the rate of thermal recovery from the surrounding medium is insignificant.

A primary control over the performance of the PFM is exerted by the diffusion length ratio $x_E/v^{1/3}$ representing the "shape" of the rock blocks bounded by flow channels. Although the shape of the response curves are identical for all magnitudes of $x_E/v^{1/3}$ the magnitudes of Q_D for which threshold behaviour is exhibited is modified. The comparative analysis further suggests an appropriate method of utilizing the two models in tandem. From knowledge of Q_D , the PFM may be utilized to determine the response corresponding to an appropriate magnitude of $x_E/v^{1/3}$. If the response is close to the lower limit of threshold behaviour, then it is established that the reservoir will deplete in a state of near thermal equilibrium. This condition is met for $Q_D = 0.0$ as illustrated in Figure 3b. With this determined it is immediately established that one of the primary assumptions of the SRM is met and, appropriately, the contribution of external heat supply may be evaluated with some confidence. The results from the 75-day circulation test at Fenton Hill illustrate this behaviour with the SRM accurately following the late thermal drawdown behaviour as illustrated in Figure 8 as contrasted with the PFM illustrated in Figure 7. This attribute is especially important as a result of the important contribution external heat supply may play in establishing the viability of HDR geothermal energy projects. For reasonable

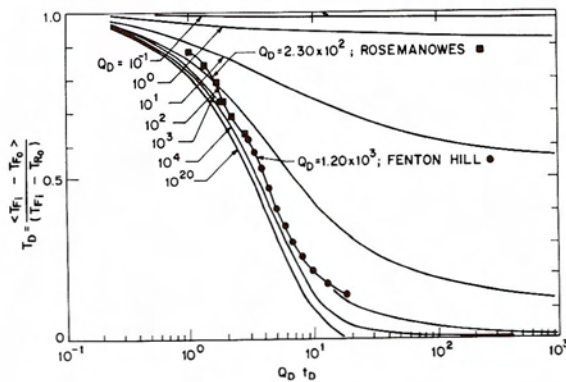


Fig. 8. Thermal drawdown data for the 75-day Fenton Hill and 1000-day Rosemanowes Quarry circulation tests compared against the Spherical Reservoir Model.

magnitudes of circulation rate, Q_D , the contribution of external heat supply and the resulting maintenance of reservoir temperatures may be anticipated to occur well within the useful lifetime of the project.

Acknowledgements

The previous represents partial results from work supported by the National Science Foundation under Grant No. MSM-8708976 and the Waterloo Centre for Groundwater Research. The sources of this support are gratefully acknowledged.

Access to data from Los Alamos Scientific Laboratory and the Camborne Geothermal Project is gratefully appreciated. Useful discussions with Bruce Robinson, Michael Fehler and Don Brown of LASL; Roy Baria and David Nicol of the Camborne Geothermal Project and Jeff Tester of MIT have contributed significantly to the work reported herein.

References

- Armstead, H.C.H. and Tester, J.W., 1987. *Heat Mining*. Spon Publishers, City p. 478.
- Elsworth, D., 1989a. Theory of thermal recovery from a spherically stimulated HDR reservoir. *J. Geophys. Res.*, 94(B2): 1927–1934.
- Elsworth, D., 1989b. Thermal recovery from multiple stimulated HDR reservoirs. *Geothermics*, 5(6): 761–774.
- Gringarten, A.C. and Witherspoon, P.A., 1973. Extraction of heat from multiple fractured dry hot rock. *Geothermics*, 2(3/4): 119–122.
- Gringarten, A.C., Witherspoon, P.A. and Ohnishi, Y., 1975. Theory of heat extraction from fractured hot dry rock. *J. Geophys. Res.*, 80(8): 1120–1124.
- Nicol, D.A.C. and Robinson, B.A., in press. Modelling the heat extraction from the Rosemanowes HDR reservoir. *Geothermics*.
- Tester, J.W. and Albright, J.N. (Editors), 1979. Hot dry rock energy extraction field test: 75 days of operation of a prototype reservoir at Fenton Hill. LANL Report LA-7771-MS, Los Alamos.